Communication

Nanostructured Crystals: Unique Hybrid Semiconductors Exhibiting Nearly Zero and Tunable Uniaxial Thermal Expansion Behavior

Jing Li, Wenhua Bi, Wooseok Ki, Xiaoying Huang, and Srihari Reddy

J. Am. Chem. Soc., **2007**, 129 (46), 14140-14141• DOI: 10.1021/ja075901n • Publication Date (Web): 30 October 2007

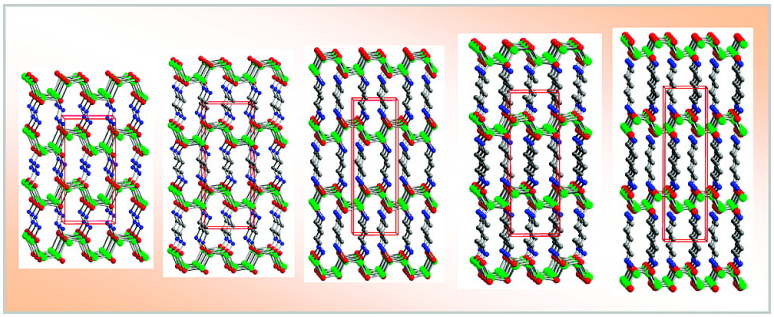

J|A|C|S
COMMUNICATIONS

Published on Web 10/30/2007

Nanostructured Crystals: Unique Hybrid Semiconductors Exhibiting Nearly Zero and Tunable Uniaxial Thermal Expansion Behavior

Jing Li,* Wenhua Bi, Wooseok Ki, Xiaoying Huang, and Srihari Reddy

Department of Chemistry and Chemical Biology, Rutgers University, 610 Taylor Road, Piscataway, New Jersey 08854

Received August 6, 2007; E-mail: jingli@rci.rutgers.edu

One of the ongoing material research concerns the chemistry and physics of inorganic−organic hybrid compounds.[1] The blending of the two components in a single structure often leads to enhancement and/or combination of useful properties originated from individual components, and more significantly, new phenomena and functionality that are not possible with the individual components alone can be induced in the blended materials. We have recently developed a unique class of nanostructured crystals with a general formula $[MQ(L)_x]$ (M = Mn, Zn, Cd; Q = S, Se, Te; L = mono- or diamine, $x = 0.5$ or 1).[2] These inorganic−organic hybrid materials possess one-, two-, and three-dimensional (1D, 2D, and 3D) extended network structures that are comprised of perfectly ordered, subnanometer sized II−VI semiconductor segments (inorganic component) and acyclic amines (organic component). They display a number of improved/enhanced physical properties over their parent bulk semiconductors, including an exceptionally broad band gap tunability (0.1−2.0 eV) and a very strong band edge absorption (e.g., 10^6 cm^{-1}), all desirable for optoelectronic applications such as photovoltaics or solid-state lighting.[3−4] In addition, the extremely strong blue shift exhibited in these systems is a result of a structure-induced quantum confinement effect (QCE), and thus, is independent of the particle size, and can be systematically tuned by modifying the crystal structure, dimensionality, and thickness of the inorganic motifs.[2]

The organic component plays an equally important role in these hybrid crystals, in shaping their conformational, structural, mechanical, and thermal properties. Herein we report nearly zero uniaxial thermal expansion behavior of a subgroup of II−VI and diamine based structures, namely 3D α-$[ZnTe(L)_{0.5}]$ [L = N_2H_4, ethylenediamine (en), propyldiamine (pda), butyldiamine (bda), and pentyldiamine (ptda)], and illustrate systematic variation of their thermal expansion properties as a function of the length of organic diamines.

A vast majority of materials respond to the change of temperature. Those that expand as the temperature increases (e.g., heating) are said to have positive thermal expansion (PTE), and those that contract upon heating are characteristic of negative thermal expansion (NTE) which are much less common. When a material is insensitive to temperature change (neither expanding nor contracting), it makes a very rare case of zero (or nearly zero) thermal expansion (ZTE).[5−7] This latter group is fundamentally very interesting and highly desirable for numerous important applications that require materials to retain a constant volume or length as temperature varies.[8a,c] Since pure isotropic ZTE materials are extremely rare, much research has been focused on developing composite materials (e.g., alloys) that combine a more commonly found PTE with a NTE component to achieve overall ZTE.[8−9] However, such composite materials often suffer from severe cracks caused by a large number of grain boundaries which will impede their performances.

Two important features make the title compounds highly attractive in minimizing such a problem. The first is that the two building blocks having distinctly different thermal properties are brought into one crystal lattice that is completely free of grain boundary issues. The bulk ZnTe shows a typical PTE behavior, while NTE was calculated for amine based structures from single-crystal data collected at two temperatures.[10] A combination of these two fragments may allow compensation of PTE and NTE effects within a uniformly ordered structure. Second, by a suitable selection of organic and inorganic components with adjustable thermal behavior, overall thermal properties of the resultant crystal lattice can be systematically tuned. The crystal structures of α-$[ZnTe(N_2H_4)_{0.5}]$ (**1**), α-$[ZnTe(en)_{0.5}]$ (**2**), α-$[ZnTe(pda)_{0.5}]$ (**3**), α-$[ZnTe(bda)_{0.5}]$ (**4**), and α-$[ZnTe(ptda)_{0.5}]$ (**5**) are shown in Figure 1. All contain single atomic slabs of ZnTe resembling a puckered honeycomb net (thickness ∼5 Å) that are interconnected by diamines via coordinative bonds between Zn and N. The insulating organic molecules act as spacers that prevent interactions between the neighboring inorganic motifs, both electronically and spatially, thus inducing a very strong quantum confinement effect. The estimated band gaps are 3.4−3.7 eV for **1**−**5**, giving rise to a huge blue shift of 1.3−1.6 eV with respect to their parent bulk ZnTe (band gap: 2.1 eV).[2,11]

Single-crystal X-ray diffraction experiments were performed on selected crystals of **1**−**5**.[11] Compounds containing diamines with an even number of carbons (n), **1** ($n = 0$), **2** ($n = 2$), and **4** ($n = 4$), crystallize in centrosymmetric space group *Pbca* (No. 61), and those with an odd number of diamines, **3** ($n = 3$) and **5** ($n = 5$), in noncentrasymmetric space group $Cmc2_1$ (No. 36). The unit cell parameters of all five structures were refined using full data sets collected at 295 K and lower temperatures.[11] Figure 2a shows the changes in the axes for **2** as an example. Clearly, two of the axes that are parallel to the inorganic layers (short axes, L_1 and L_2) respond positively to the increase of temperature for all five compounds, with their thermal expansion coefficients (α) varying between $(0.9−1.5) \times 10^{-5}$ K^{-1} and $(1.4−2.9) \times 10^{-5}$ K^{-1} for L_1 and L_2, respectively. The extent of their PTE is, however, generally decreases as n increases, as shown in Figure 2c for L_2 (L_1 behaves similarly). The axis perpendicular to the ZnTe layers (long axis, L_3) exhibits a significantly smaller thermal expansion (Table 1). For **1** with the shortest diamine ($n = 0$), L_3 features a very small but positive thermal expansion. For higher n, L_3 shows NTE with increasing magnitude as diamine gets longer (Figure 2b,c). The effect of the organic molecule is further illustrated in Figure 2d, taking **1** ($n = 0$, even) and **3** ($n = 3$, odd) as examples. PTE is observed in the inorganic layer for both compounds, while the organic layer shows a negative effect with an increasing scale as n increases. It is this difference in the thermal behavior of the two structure motifs that leads to the sign and magnitude change of α.

10.1021/ja075901n CCC: $37.00

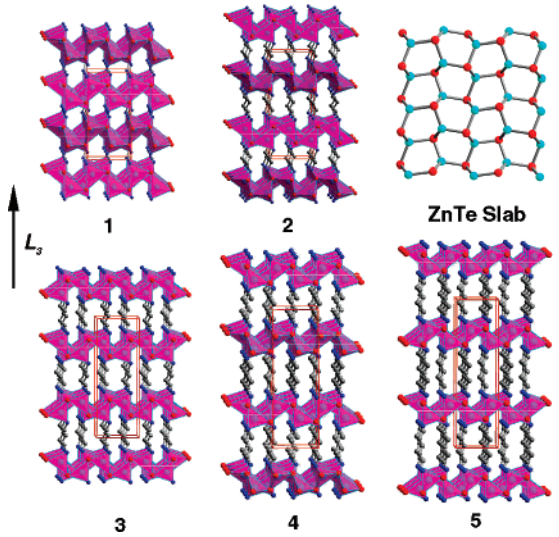

Figure 1. Crystal structures of **1**−**5** and the ZnTe single-atomic slab. The light-blue balls inside tetrahedral are Zn; red balls, Te; dark blue balls, N; gray balls, C. Hydrogen atoms are omitted for clarity. For **1**, **2**, and **4**, the view is along the *b*-axis, and for **3** and **5**, it is along the *c*-axis. L_3 (the long axis) is the inorganic−organic stacking axis (perpendicular to II−VI layers).

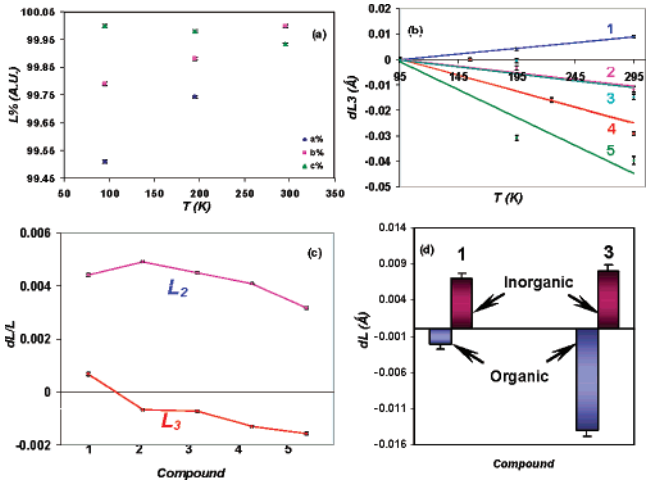

Figure 2. (a) Relative change in the unit cell constants for **2** ($a = L_2$, $b = L_1$, $c = L_3$) as a function of temperature; (b) Change in L_3 as a function of T(K) for **1**−**5** (top down. Lines are drawn to guide the eyes); (c) Normalized change in L_2 and L_3 for **1**−**5**; and (d) Change in the inorganic (brown) and organic (blue) layer along L_3 for **1** and **3** between 95 and 295 K (all with *error bars*).

Table 1. L_3(295 K), ΔL_3(295 K, 95 K), and Thermal Expansion Coefficient (α) of L_3 Calculated by Linear Regression Method

compound (*n*)	L_3/Å (295 K)	ΔL_3/Å (L_3,295K − L_3,95K)	$\alpha \times 10^6$/K^{-1}
$[ZnTe(N_2H_4)]_{0.5}$ (0)	13.3114(15)	+0.009	+3.759
$[ZnTe(en)]_{0.5}$ (2)	17.5569(10)	−0.0117	−3.415
$[ZnTe(pda)]_{0.5}$ (3)	20.2234(13)	−0.0146	−3.459
$[ZnTe(bda)]_{0.5}$ (4)	22.3575(11)	−0.029 (155K)	−8.929
$[ZnTe(ptda)]_{0.5}$ (5)	25.2744(18)	−0.0396	−7.901

A linear response theory has been employed to calculate the phonon spectrum of a prototype hybrid structure β-$[ZnTe(en)_{0.5}]$[12] to study and understand possible mechanisms. The calculations show that a number of transverse and transverse-longitudinal (mixed) modes can be excited in the temperature range 4−400 K. Their frequencies are in the region similar to the transverse modes found in other materials that contribute to NTE.[13] The frequency red shift with lowering temperature (a signature of the transverse mode) has also been confirmed by Raman experiments.

There are only a few exceptions of known NTE or ZTE materials that are not insulators.[5] Semiconducting materials that combine ZTE and other useful electronic and optical properties are in high demand. The title compounds represent a remarkable group of nanostructured hybrid semiconductor materials that are not only capable of tuning electronic and optical properties but also competent in achieving desired thermal expansion properties by tailoring two distinctly different structural components in a single crystal lattice.

Acknowledgment. Financial support from the National Science Foundation (Grant No. DMR-0422932) is gratefully acknowledged. We thank Dr. Y. Zhang for helpful discussions.

Supporting Information Available: Details of synthesis, crystallographic details, structure analysis, unit cell parameters, and other related materials. This material is available free of charge via the Internet at http://pubs.acs.org.

References

(1) (a) Mitzi, D. B. In *Progress in Inorganic Chemistry*; Karlin, K. D., Ed.; John Wiley & Sons, Inc.: 1999; p 1. (b) *Handbook of organic-inorganic hybrid materials and nanocomposites*; Nalwa, H. S.; American Scientific Publishers: 2003. (c) Coronado, E.; Palomares, E. *J. Mater. Chem.* **2005**, *15*, 3559.
(2) (a) Huang, X.-Y.; Li, J.; Fu, H. *J. Am. Chem. Soc.* **2000**, *122*, 8789. (b) Huang, X.-Y.; Li, J.; Zhang, Y.; Mascarenhas, A. *J. Am. Chem. Soc.* **2003**, *125*, 7049. (c) Huang, X.-Y.; Li, J. *J. Am. Chem. Soc.* **2007**, *129*, 3157.
(3) (a) Fluegel, B.; Zhang, Y.; Mascarenhas, A.; Huang, X.-Y.; Li, J. *Phys. Rev. B* **2004**, *70*, 205308/1. (b) Zhang, Y.; Dalpian, G. M.; Fluegel, B.; Wei, S.-H.; Mascarenhas, A.; Huang, X.-Y.; Li, J.; Wang, L.-W. *Phys. Rev. Lett.* **2006**, *96*, 026405.
(4) (a) Fu, H.-X.; Li, J. *J. Chem. Phys.* **2004**, *14*, 6721. (b) Moon, C.-Y.; Dalpian, G. M.; Zhang, Y.; Wei, S.-H.; Huang, X.-Y.; Li, J. *Chem. Mater.* **2006**, *18*, 2805.
(5) Salvador, J. R.; Guo, F.; Hogan, T.; Kanatzidis, M. G. *Nature* **2003**, *425*, 702. Sleight, A. *Nature* **2003**, *425*, 674.
(6) Margadonna, S.; Prassides, K.; Fitch, A. N. *J. Am. Chem. Soc.* **2004**, *126*, 15390.
(7) Roy, R.; Agrawal, D. K.; McKinstry, H. A. *Annu. Rev. Mater. Sci.* **1989**, *19*, 59.
(8) (a) Evans, J. S. O.; Hu, Z.; Jorgensen, D. D.; Argyriou, D. N.; Short, S.; Sleight, A. W. *Science* **1997**, *275*, 61. (b) Mary, T. A.; Evans, J. S. O.; Vogt, T.; Sleight, A. W. *Science* **1996**, *272*, 90. (c) Sleight, A. W. *Annu. Rev. Mater. Sci.* **1998**, *28*, 29. (d) Sleight, A. W. *Inorg. Chem.* **1998**, *37*, 2854. (e) Attfield, M. P.; Sleight, A. W. *Chem. Mater.* **1998**, *10*, 2013. (f) Evans, J. S. O.; Hanson, P. A.; Ibberson, R. M.; Duan, N.; Kameswari, U.; Sleight, A. W. *J. Am. Chem. Soc.* **2000**, *122*, 8694. (g) Li, J.; Yokachi, A.; Amos, T. G.; Sleight, A. W. *Chem. Mater.* **2002**, *14*, 2602.
(9) (a) Evans, J. S. O. *J. Chem. Soc., Dalton Trans.* **1999**, 3317. (b) Villaescusa, L. A.; Lightfoot, P.; Teat, S. J.; Morris, R. E. *J. Am. Chem. Soc.* **2001**, *123*, 5453. (c) Barrera, G. D.; Bruno, J. A. O.; Barron, T. H. K.; Alan, N. L. *J. Phys.: Condens. Matter* **2005**, *17*, R217.
(10) (a) Babu, A. M.; Weakley, T. J. R.; Murthy, M. R. N. *Z. Kristallogr. New Cryst. Struct.* **1998**, *213*, 321. (b) Vaidhyanathan, R.; Natarajan, S.; Rao, C. N. R. *J. Mol. Struct.* **2002**, *608*, 123.
(11) Suitable sized single crystals of **1**−**5** were selected and carefully mounted on top of glass fibers. The data collections for the unit cell measurements and structure refinements were carried out on a Siemens SMART APEX I diffractometer (Mo Kα, $\lambda = 0.717\,03$ Å) with a CCD area detector and graphite monochromator. The crystals were centered in the beam and cooled by a liquid-nitrogen cryostream. The unit cell parameters were determined by general least-square refinement using full data sets collected at 95, 195, and 295 K for **1**−**3** and **5** (SMART software). For **4**, a full set of data collected at 155, 225, and 295 K were used for unit cell refinement due to a phase transition that occurred below 150 K. All structures were solved by direct method and refined by full matrix least-square based on F^2 by using the program package of SHELXTL.
(12) Zhang, Y.; Islam, Z.; Ren, Y.; Parilla, P. A.; Ahrenkiel, S. P.; Lee, P. L.; Mascarenhas, A.; McNevin, M. J.; Naumov, I.; Fu, H.-X.; Huang, X. Y.; Li, J. *Phy. Rev. Lett.* **2007**, *99*. Also see the Supporting Information.
(13) (a) Hancock, J. N.; Turpen, C.; Schlesinger, Z. et al. *Phys. Rev. Lett.* **2004**, *93*, 225501. (b)Chapman, K. W.; Hagen, M.; Kepert, C. J.; Manuel, P. *Physica B* **2006**, *385*, 60.

JA075901N